

First-principles study of magnetism of 3d transition metals and nitrogen co-doped monolayer MoS₂*

Long Lin(林龙)¹, Yi-Peng Guo(郭义鹏)¹, Chao-Zheng He(何朝政)^{2,†}, Hua-Long Tao(陶华龙)³,
Jing-Tao Huang(黄敬涛)¹, Wei-Yang Yu(余伟阳)⁴, Rui-Xin Chen(陈瑞欣)¹,
Meng-Si Lou(娄梦思)¹, and Long-Bin Yan(闫龙斌)¹

¹Cultivating Base for Key Laboratory of Environment-Friendly Inorganic Materials in Henan Province, School of Materials Science and Engineering, Henan Polytechnic University, Jiaozuo 454000, China

²Institute of Environmental and Energy Catalysis, School of Materials Science and Chemical Engineering, Xi'an Technological University, Xi'an 710021, China

³Liaoning Key Materials Laboratory for Railway, School of Materials Science and Engineering, Dalian Jiaotong University, Dalian 116028, China

⁴School of Physics and Electronic Information Engineering, Henan Polytechnic University, Jiaozuo 454003, China

(Received 12 April 2020; revised manuscript received 14 May 2020; accepted manuscript online 28 May 2020)

The electronic structures and magnetic properties of diverse transition metal ($TM = \text{Fe, Co, and Ni}$) and nitrogen (N) co-doped monolayer MoS₂ are investigated by using density functional theory. The results show that the intrinsic MoS₂ does not have magnetism initially, but doped with TM ($TM = \text{Fe, Co, and Ni}$) the MoS₂ possesses an obvious magnetism distinctly. The magnetic moment mainly comes from unpaired Mo:4d orbitals and the d orbitals of the dopants, as well as the S:3p states. However, the doping system exhibits certain half-metallic properties, so we select N atoms in the V family as a dopant to adjust its half-metal characteristics. The results show that the (Fe, N) co-doped MoS₂ can be a satisfactory material for applications in spintronic devices. On this basis, the most stable geometry of the (2Fe–N) co-doped MoS₂ system is determined by considering the different configurations of the positions of the two Fe atoms. It is found that the ferromagnetic mechanism of the (2Fe–N) co-doped MoS₂ system is caused by the bond spin polarization mechanism of the Fe–Mo–Fe coupling chain. Our results verify that the (Fe, N) co-doped single-layer MoS₂ has the conditions required to become a dilute magnetic semiconductor.

Keywords: MoS₂, first principle calculations, diluted magnetic semiconductors, magnetic property

PACS: 71.15.Mb

DOI: 10.1088/1674-1056/ab9741

1. Introduction

Since the discovery of graphene,^[1] there has been a growing interest in atomically thin two-dimensional (2D) crystals for potential applications in next-generation nanoelectronic devices.^[2–5] Layered transition metal dichalcogenides (TMDs) represent a class of material that can be shaped into monolayers, which display distinct physical properties from their bulk counterpart.^[6] Monolayer MoS₂, as a new type of 2D material, has gradually aroused considerable interest in the past few decades, due to its unique physical, chemical, optical, and mechanical properties. The interest originates from its high surface-to-volume ratio comparable to the surface-to-volume ratio of graphene, indirect-to-direct band-gap, and layer-dependent tunable band-gap. The MoS₂ exhibits its enormous potential applications in the field of transistor,^[7] field-effect transistor (FET),^[8] photocatalytic degradation,^[9] hydrogen production,^[10] gas sensor,^[11] solar cells,^[12] and photodetector.^[13] The electronic properties of MoS₂ strongly

depend on the layer thickness. Bulk MoS₂ has an indirect band-gap of 1.2 eV, and the MoS₂ has a direct band-gap of about 1.9 eV.^[14]

Owing to the potential applications and the great demands for MoS₂ nanostructures, a variety of methods have been developed and explored in the past few years. Particularly, recent research showed that TM elements-doped MoS₂ could drastically enhance the chemical activity and the sensitivity as the doped atoms could effectively regulate and control the electronic structures and magnetic properties. Komsa *et al.*^[15] found it possible to control the creation of vacancy by using electron irradiation or low-energy argon sputtering and then the vacancies are filled with substitutional impurity atoms. Suh *et al.*^[16] investigated the effect of niobium (Nb) doping on the crystal structure, electronic and optical properties of MoS₂, and proved that Nb doping can improve the electromagnetic properties of MoS₂ materials. Fan *et al.*^[17] studied the structure and electronic properties of MoS₂ doped with differ-

*Project supported by the Key Project of the National Natural Science Foundation of China (Grant No. 51702089), the National Natural Science Foundation of China (Grant Nos. 21603109 and 11804081), the Henan Joint Fund of the National Natural Science Foundation of China (Grant No. U1404216), China Postdoctoral Science Foundation (Grant No. 2019M652425), the One Thousand Talent Plan of Shaanxi Province, China, the Natural Science Foundation of Henan Province, China (Grant Nos. 182102210305 and 19B430003), the Key Research Project for the Universities of Henan Province, China (Grant No. 19A140009), the Doctoral Foundation of Henan Polytechnic University, China (Grant No. B2018-38), the Open Project of Key Laboratory of Radio Frequency and Micro-Nano, and the Fund from the Electronics of Jiangsu Province, China (Grant No. LRME201601).

†Corresponding author. E-mail: hecz2019@xatu.edu.cn

ent *TM* elements in S vacancies, as well as the adsorption of various gas molecules. Their results showed that embedded Fe and Co significantly changed the electronic and magnetic properties of the single-layer MoS₂, and had better adsorption properties on gas molecules than those doped with other *TM* elements. Zhang *et al.*^[18] discussed the electronic properties of MoS₂ doped by non-metallic elements with different doping concentrations. The calculation results showed that P atoms made the system to present p-type characteristic. In contrast, Cl was considered as a suitable n-type dopant. Ramasubramanian and Naveh^[19] investigated the electronic and magnetic properties of Mn-doped monolayer MoS₂. They demonstrated the potential for engineering a new class of atomically thin diluted magnetic semiconductor (DMS) based on Mn-doped MoS₂. Zhao^[20] investigated the magnetic properties of Re atom doped single-layer MoS₂ by first-principles calculation, and found that Re doping can effectively improve the magnetic properties of MoS₂. Cui *et al.*^[21] predicted the adsorption performances of Pd-MoS₂ for H₂, CH₄, and C₂H₂, and found that the Pd-MoS₂ has good adsorption and desorption performance, and is a satisfactory C₂H₂ and H₂ sensing material, but not suitable for detection methane gas. Cheriyan *et al.*^[22] studied the electronic and optical properties of monolayers of MoS₂ doped by N, Co, and co-doped by (Co, N) for visible light photocatalytic activity by using density functional theory (DFT). The observed results showed that intrinsic MoS₂ was highly suitable for visible light photocatalytic dye degradation compared with N-doped MoS₂. Garandel *et al.*^[23] investigated the hcp Co (0001)/MoS₂ interface electronic struc-

ture by first-principles calculations based on the DFT. They demonstrated that the Co-doped system became metallic due to hybridization between Co:3d and S:3p orbitals. At present, the doping of MoS₂ has been widely studied.^[24–28] However, as far as we know, there are few studies about the electronic structures and magnetic properties of the transition state atoms and nonmetallic atoms co-doped MoS₂. Therefore, it is necessary to study the electromagnetic properties of (*TM*, N) co-doped MoS₂ systematically.

In this research, we propose (*TM*, N) (*TM* = Fe, Co, and Ni) co-doped MoS₂ as a promising DMSs material. We calculate *TM*-doped MoS₂ and (*TM*, N) co-doped MoS₂ systems. The effects of Fe, Co, and Ni dopants on the electronic structures and magnetic properties of (*TM*, N) co-doped MoS₂ system are investigated. We further study the possible structure of (2Fe, N) co-doped MoS₂, and obtain a most stable structure.

2. Computational details and models

MoS₂ belongs to the *P6₃/mmc* space group, the lattice constant calculated here was 3.15 Å, which is in agreement with the experimental result.^[29] According to the unit cell, we calculate *TM*-doped and (*TM*, N) co-doped MoS₂ by using the 4 × 4 × 1 supercell cleaved through (0 0 1) surface of bulk material, which includes 16 Mo atoms and 32 S atoms with a vacuum range of 10 Å as shown in Fig. 1. A previous report^[30] demonstrated that the size of the supercell is sufficient to study the discrete doping geometry and co-doping geometry, while a 10-Å slab can prevent interaction between adjacent units and isolate the interaction between dopants.^[31] Figure 1 shows the

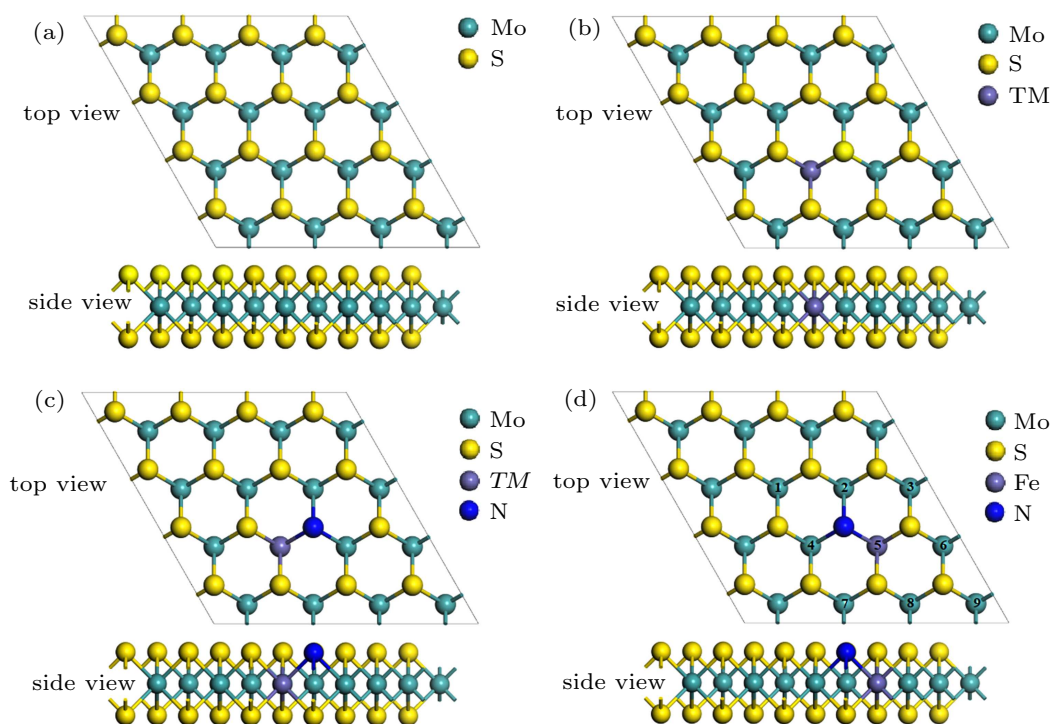


Fig. 1. Structure of the supercell used for the calculation, showing top view and side view of (a) intrinsic MoS₂, (b) *TM*-MoS₂, (c) (*TM*, N) co-doped MoS₂ and (d) (2Fe, N) co-doped MoS₂, respectively. Mo atoms replace Fe atoms, which is indicated by 1–9.

vertical view and lateral view of the optimized MoS₂ supercell structure: figure 1(a) shows intrinsic MoS₂; figure 1(b) shows *TM*-MoS₂, figure 1(c) is the structure of (*TM*, N) co-doped MoS₂, and figure 1(d) shows the structure of (2Fe, N) co-doped MoS₂. As shown in Fig. 1(d), the Mo atoms replaces the Fe atoms, which is indicated by numbers 1–9.

The structural optimization and electronic structures were calculated in this work by using Cambridge Serial Total Energy Package (CASTEP) package based on the density functional theory (DFT) method.^[32] We used the Perdew–Brueke–Ernzerh (PBE) function of the Generalized Gradient Approximation (GGA) to calculate the exchange and related energy.^[33,34] The *k*-point sample of the Monkhorst–Pack grid was sampled to $3 \times 3 \times 1$ of the Brillouin-zone integration and the plane wave cutoff energy was set to be 500 eV for geometric optimization and electronic structure calculations. We selected the convergence criteria of the energy as 1×10^{-5} eV/atom. All atoms were allowed to relax completely until any force is less than 0.05 eV/Å, the maximum atom displacement is 0.002 Å, and the stress is not more than 0.1 GPa to ensure accurate results for the total energy.^[35–37]

3. Results and discussion

3.1. Intrinsic MoS₂

Prior to studying different types of doping systems, we first study the electronic structures and magnetic properties of the intrinsic MoS₂ monolayers. For the intrinsic MoS₂, the optimized lattice constants of the supercell are $a = b = 12.72$ Å and $c = 13.12$ Å. Our calculation results are close to the results of the non-optimized MoS₂, indicating that the calculations are accurate. Then we calculate the total intrinsic density of states (TDOS) and partial density of states (PDOS) of pure MoS₂. The calculation results show that the intrinsic MoS₂ is non-magnetic. In the meantime, we also calculate its energy band structure. The calculated results obtained after relaxation, display that band structure of intrinsic MoS₂ (Fig. A1 in Appendix A) shows a bandgap of 1.846 eV, which approximates to the experimental result of 1.88 eV.^[38] In the perfect case, the valence band minimum (CBM) and the valence band maximum (VBM) are both at *K* point, therefore the bandgap is direct and in good agreement with previously reported results.^[39]

3.2. *TM* (Fe, Co, and Ni)-doped MoS₂ monolayers

We first calculate the electronic structures of *TM*-doped MoS₂ monolayers. The doping concentration of *TM* is 6.25 at.% as shown in Fig. 1(b). The calculation results are shown in Table 1. It shows that S–*TM* bond length is shorter than S–Mo bond length ($d_{S-Fe} = 2.283$ Å, $d_{S-Co} = 2.293$ Å, $d_{S-Ni} = 2.405$ Å, and $d_{S-Mo} = 2.408$ Å). These differences

can be attributed to the fact that the atomic radius of Fe, Co, and Ni atoms are smaller than that of the Mo atom. Then we calculate the band populations of *TM*-doped MoS₂. The results show that the total magnetic moment of Fe-doped MoS₂ is $2.02 \mu_B$, and the local magnetic moment of Fe atom is $1.17 \mu_B$. The total magnetic moment of Co-doped MoS₂ is $2.93 \mu_B$, and the local magnetic moment of Co atom is $0.86 \mu_B$. The total magnetic moment of Ni-doped MoS₂ is $4.05 \mu_B$, and the local magnetic moment of the Ni atom is $1.11 \mu_B$. As can be seen from the data in Table 1, the magnetism of *TM*-doped MoS₂ system mainly comes from the doped *TM* atoms.

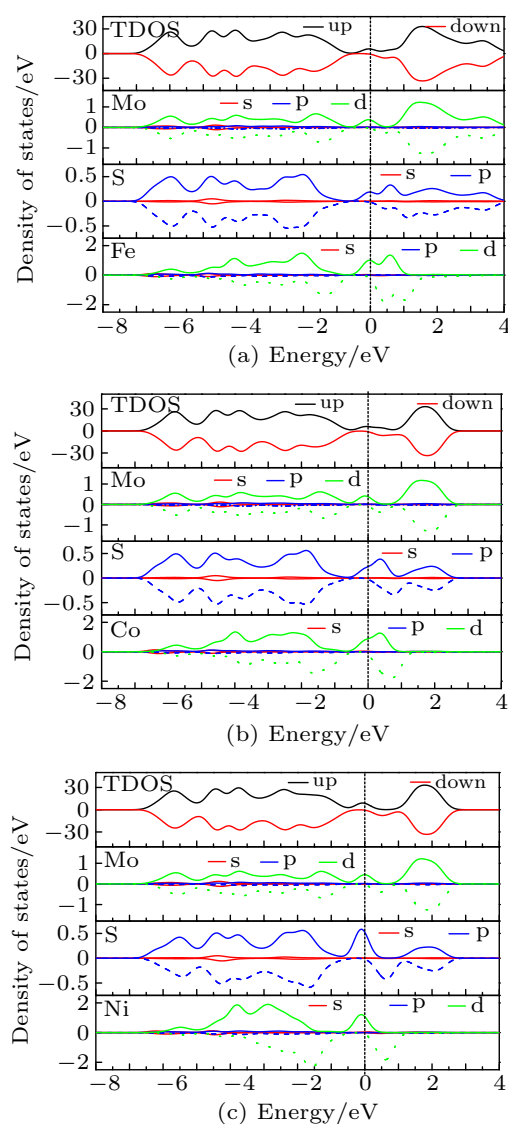


Fig. 2. TDOS and PDOS for (a) Fe, (b) Co, and (c) Ni-doped MoS₂, calculated by using PBE functional, with Fermi level set to be 0 eV.

Next, we calculate the total density of states (TDOS) and partial density of states (PDOS) of *TM*-doped MoS₂ as shown in Fig. 2. Figure 2 shows the TDOS of *TM*-doped MoS₂ system and the PDOS of *TM* dopants and *TM* atom nearest Mo and S atoms. From Fig. 2 it can be easily determined that TDOS is mainly contributed to by *TM*:3d, Mo:4d, and S:2p

orbitals near the Fermi level. To further understand the effect of TM doping on the electronic structure of MoS_2 , we also calculate the band structure of the TM -doped MoS_2 system as shown in Fig. A2 in Appendix A. It can be seen from Fig. A2 that the TM -doped MoS_2 system exhibits the half-metallicity to a certain degree, which can also be found from the density of states.

Table 1. Calculation results of intrinsic MoS_2 and TM -doped MoS_2 , S–Mo, and S–TM bond lengths, and total magnetic moment, and magnetic moment of S, Mo, and TM atoms, respectively.

Dopant site	Bond length/Å		Magnetic moments/ μ_B			
	d_{S-Mo}	d_{S-TM}	Total	S	Mo	TM
MoS_2	2.408	–	0.00	0.00	0.00	–
Fe	2.412	2.283	2.02	0.01	0.13	1.17
Co	2.416	2.293	2.93	0.04	0.30	0.86
Ni	2.398	2.405	4.05	0.29	0.16	1.11

3.3. (TM , N) co-doped MoS_2 monolayers

There are few studies of the electronic structures and magnetic properties of the MoS_2 co-doped with transition atoms and nonmetallic atoms. Therefore, in this subsection, we will continue to study the electronic structures and magnetic properties of (TM , N) co-doped MoS_2 . The structure is shown in Fig. 1(c), in which an S atom in MoS_2 is replaced with an N atom, then one TM atom is doped in the adjacent Mo position, and doping concentration is 6.25 at.%. The calculation results are shown in Table 2. To determine the stability of the (TM , N) co-doped MoS_2 system, we calculate the formation energy of the three doping systems.

The formation energy formula is calculated to be^[40,41]

$$E_{\text{form}} = E_{\text{doped}} - E_{\text{intrinsic}} - \mu_{TM} - \mu_N + \mu_{Mo} + \mu_S, \quad (1)$$

where E_{doped} and E_{MoS_2} are the total energy of (TM , N) co-doped MoS_2 and intrinsic one, respectively; μ_{TM} , μ_N , μ_{Mo} , and μ_S are the chemical potentials for the TM dopant, N atom, Mo host, and S host, respectively. Their specific values are obtained from the stable element of the corresponding element. Co and Ni elemental chemical potential are obtained from a faced-centered cubic structure (fcc), and the chemical potential of Fe is obtained from the body-centered cubic (bcc) structure. The formation energy of MoS_2 itself, $E_{\text{form}}(MoS_2)$, can be calculated from the expression

$$E_{\text{form}} = \mu_{MoS_2} - \mu_{Mo}^0 - 2\mu_S^0, \quad (2)$$

where μ_{MoS_2} is equal to E_{pure} per MoS_2 formula unit, and μ_{Mo}^0/μ_S^0 is the total energy per atom of Mo/S in its reference phase. For Mo, the reference phase is the bulk bcc metal. The reference phase for S is the S8 ring, which is the most stable state at room temperature. The value of μ_{Mo} and μ_S

depend on the experimental growth conditions. For the Mo-rich case, the Mo chemical potential is equal to the bulk Mo value, $\mu_{Mo}^{\text{Mo-rich}} = \mu_{Mo}^0$, and the S chemical potential can be obtained from $\mu_{MoS_2} = \mu_{Mo} + 2\mu_S$ based on thermodynamic equilibrium. Therefore, combined with Eq. (2), the chemical potentials for the Mo-rich limit can then be written as

$$\mu_{Mo}^{\text{Mo-rich}} = \mu_{Mo}^0, \quad (3)$$

$$\mu_S^{\text{Mo-rich}} = \mu_S^0 + \frac{1}{2}E_{\text{form}}(MoS_2). \quad (4)$$

Likewise, under S-rich conditions, the values are

$$\mu_{Mo}^{\text{S-rich}} = \mu_{Mo}^0 + E_{\text{form}}(MoS_2), \quad (5)$$

$$\mu_S^{\text{S-rich}} = \mu_S^0. \quad (6)$$

All of the formation energy values are listed in Table 2.

The calculation results show that the formation energy of the (Fe, N) co-doped MoS_2 system is the smallest in the three systems, indicating that the (Fe, N) configuration is the most stable. The length of the Fe–N bond is 1.965 Å. The total magnetic moment of (Fe, N) co-doped MoS_2 system is 1.00 μ_B , and the local magnetic moment of doped Fe atom is 0.64 μ_B . From the data in Table 2, we can see that the formation energy values of (Fe, N), (Co, N), and (Ni, N) co-doped MoS_2 system are all higher than 0, indicating that the formation of these systems requires energy absorption. We further calculate the band structure for each of (Fe, N), (Co, N), and (Ni, N) co-doped MoS_2 . In Fig. A3, the bandgap of (Co, N) co-doped MoS_2 is 0.042 eV, which is smaller than that of (Fe, N) co-doped MoS_2 . It can be seen from Figs. A1 and A2 that the introduction of N atom regulates the half-metallic properties of Fe-doped MoS_2 system, which is consistent with our research requirements. According to the above reasons, we choose the (Fe, N) co-doped MoS_2 system as the project of further study.

Table 2. Calculation results of (TM , N) co-doped MoS_2 , TM –N bond length, total magnetic moment, the local magnetic moment of TM atom, and formation energy.

Dopant site	$d_{TM-N}/\text{Å}$	Total/ μ_B	TM/μ_B	$E_{\text{form}}/\text{eV}$	
				Mo-rich	S-rich
Fe	1.965	1.00	0.64	2.64	–0.06
Co	1.975	1.98	0.73	3.91	1.21
Ni	1.939	1.11	0.18	4.72	2.22

Next, we come to analyze the TDOS and PDOS for (Fe, N) co-doped MoS_2 , and the results are presented in Fig. 3(a). Due to the doping of TM and N atoms, some new impurity state energy levels are introduced into the energy gap. It can be seen that the valence band (from –8 eV to –1 eV) mainly comes from Fe:3d, Mo:4d, S:3p, and N:2p orbitals, while Fe:4s, Mo:5s, S:3s, and N:2s orbitals contribute less. We can see that (Fe, N) TDOS co-doped MoS_2 is asymmetric. It can be seen from Table 2 that the system has a total magnetic moment of about 1.00 μ_B . The doping Fe atom plays a great role in contributing the magnetic moment.

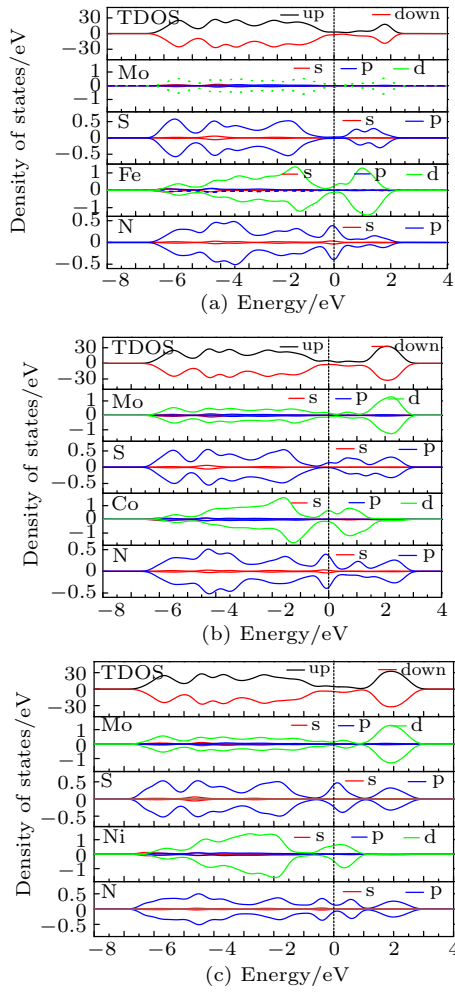


Fig. 3. TDOSs and PDOSs for (a) Fe-N, (b) Co-N, and (c) Ni-N co-doped monolayer MoS₂, with Fermi level set to be 0 eV.

Table 3. Calculation results of 8 configurations for (2Fe, N) co-doped MoS₂. Fe-Fe distance, ΔE , ΔE_{FM} , total magnetic moment, and magnetic moment of Fe₁, Fe₂, N, Mo, and S atoms, respectively.

Configuration	d (Fe-Fe)/Å		ΔE /eV	ΔE_{FM} /meV	Magnetic moment/ μ_{B}					
	AFM	FM			Total	Fe ₁	Fe ₂	N	Mo	S
(2, 4)	3.286	3.294	–	42.5	3.26	1.77	1.77	–0.03	–0.01	–0.06
(1, 2)	3.428	3.425	–0.48	2.2	3.00	1.96	1.74	–0.09	–0.10	0.00
(2, 6)	5.255	5.275	0.68	–4.8	3.40	2.05	2.05	0.03	–0.01	0.00
(1, 5)	5.495	5.487	0.14	–29.1	3.02	1.87	1.80	–0.06	0.38	–0.05
(3, 8)	5.535	5.508	0.59	–1.1	3.32	1.81	1.78	–0.01	–0.04	0.00
(1, 3)	6.289	6.242	–0.68	64.2	3.47	1.85	1.85	–0.03	0.04	0.00
(3, 7)	6.253	6.280	0.33	–92.3	3.44	2.08	2.03	–0.02	0.01	0.00
(1, 9)	10.923	10.918	0.38	–14.8	3.05	1.84	1.85	–0.08	0.00	0.00

It can be seen that the magnetic properties and lattice parameters of different Fe dopants in MoS₂ configuration are different from those listed in Table 3. Next, we study the different atomic structures of a single layer of MoS₂ doped with two Fe atoms. For a series of (2Fe, N) co-doped MoS₂, the (1, 3) configuration has the minimum ΔE (–0.68 eV), the maximum ΔE_{FM} (64.2 meV) and the largest total magnetic moment (3.47 μ_{B}). The local magnetic moment for each of Fe₁ atom

3.4. (2Fe, N) co-doped MoS₂

The previous studies indicated the substitutional dopant at the Mo site, and did not take into account the atomic complexes due to being doped with more atoms. We put more thought into the effect of the doping concentration on the properties of materials. After studying the electromagnetic properties of *TM*-doped MoS₂ and (*TM*, N) co-doped MoS₂, we continue to study the magnetic source of (Fe, N) co-doped single-layer MoS₂ system. We increase the doping concentration of Fe atoms in the (Fe, N) co-doping MoS₂ system to 12.5 at.%, by replacing two Mo atoms in MoS₂ with two Fe atoms as shown in Fig. 1(d). In Fig. 1(d), one N atom is fixed, and two Mo atoms marked by numbers 1–9 replace the two Fe atoms. The calculation results are shown in Table 3. Select the (2, 4) configuration with the smallest d (Fe-Fe) as the benchmark, and calculate the total energy difference (ΔE) between different configurations and (2, 4) configuration in Table 3, then we will use the energy differences between ferromagnetic (FM) and antiferromagnetic (AFM) states ($\Delta E_{\text{FM}} = E_{\text{AFM}} - E_{\text{FM}}$), which have been calculated in (2Fe, N) co-doped MoS₂, to determine the magnetic coupling between the two Fe atoms. The Fe-Fe distance value after relaxation under AFM and FM, ΔE , ΔE_{FM} , the total magnetic moment of (2Fe, N) co-doped MoS₂ system, and local magnetic moment of Fe₁, Fe₂, N, Mo, and S atoms are all listed in Table 3.

and that of Fe₂ atom is 1.85 μ_{B} , and the local magnetic moment of N atom is –0.03 μ_{B} . The (1, 3) configuration has the lowest energy, indicating that it is the most stable structure and has stable ferromagnetism.

Next, we calculate the TDOS and PDOS for (1, 3) configuration for investigating the magnetic origin in these systems, which is depicted in Fig. 4. From Fig. 4, we can see that the band structure around the Fermi level is derived mainly

from Fe:3d, Mo:4d, and S:3p orbitals, although there are also small contributions in the valence band from Fe:3p, Mo:4p, S:3s, Fe:4s, Mo:5s, and N:2s orbitals. The magnetism can be explained by the direct magnetic coupling mechanism of d orbitals. Since Fe and Fe atoms are close to each other, the wave functions of d orbitals may overlap to some extent, which enables the hybridization of d orbitals in both Fe and Mo atoms. We also calculate the band structure of (1, 3) configuration as shown in Fig. A4. As can be seen from Fig. A4, the (2Fe, N) co-doped MoS₂ material is a direct bandgap semiconductor. The bandgap is 0.505 eV.

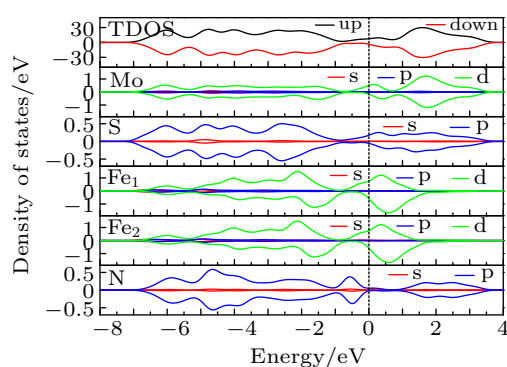


Fig. 4. TDOSs and PDOSs for (2Fe, N) co-doped monolayer MoS₂, with Fermi level set to be 0 eV.

To further study the magnetic generation mechanism of (2Fe, N) co-doped MoS₂ system, we calculate the spin-charge density of the doping system and analyze the charge transfer of each atom in the system, and the results are shown in Fig. 5.

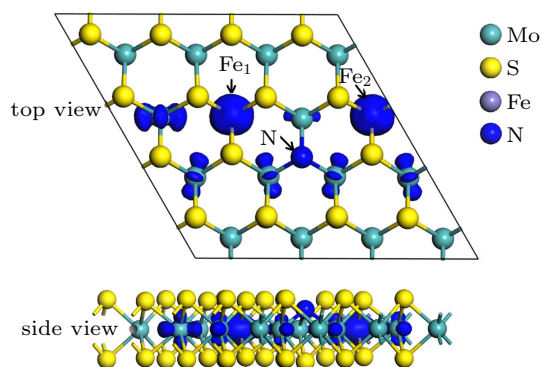


Fig. 5. Spin density distribution of (2Fe, N) co-doped MoS₂ in FM coupling, with isovalue set to be $0.02 e/\text{\AA}^3$.

The three-dimensional (3D) iso-surface possesses a spin-charge density of $0.02 e/\text{\AA}^3$. According to the results, we find that spin-polarized states are localized around the Fe atoms in the configuration of (2Fe, N) co-doped MoS₂. We can see that the blue range with Fe₁, Fe₂, and N. It shows that the doped Fe atoms play a major role in the magnetic moment of the system, and the three Mo atoms around the N atoms play a secondary role. From Fig. 5, we infer that the Fe₁:3d–Mo:4d–Fe₂:3d coupling chain is the reason why the (2Fe, N) co-doped MoS₂

system produces magnetism. Classically, the spin-polarized states are not located in the Fe–Fe system, which may induce magnetic order.

4. Conclusions

We systematically studied the electronic structures and magnetic properties of MoS₂ induced by *TM* and N dopants based on density functional theory. The results show that the *TM* atoms Fe, Co, and Ni-doped MoS₂ are magnetic, and the local magnetic moment mainly comes from the contribution of doped atoms. The (*TM*, N) co-doped MoS₂ also has magnetic properties, and the doping of the N atom regulates the half-metallic nature of the doping system. The doping system has both semiconductor properties and certain magnetic properties, which is beneficial for practical application as a dilute magnetic semiconductor. Among them, (Fe, N) co-doped MoS₂ has the best electromagnetic properties. The total magnetic moment of the (2Fe, N) co-doped single-layer MoS₂ is $3.47 \mu_B$, and the maximum local magnetic moment for each of two Fe atoms is $1.85 \mu_B$. The spin polarization of the system is mainly contributed by two doped Fe atoms, which indicates that the Fe atoms in the MoS₂ lattice are localized. It can be concluded that the main contributions of magnetism come from Fe:3d, Mo:4d, S:3p, and N:2p orbitals. The research results have a certain reference value for experimental verification and practical application.

Acknowledgment

Computational resources were provided by the Henan Polytechnic University High-performance Grid Computing Platform.

Appendix A: Supporting materials

Band structures of *TM*-doped MoS₂ system are shown in the following figures.

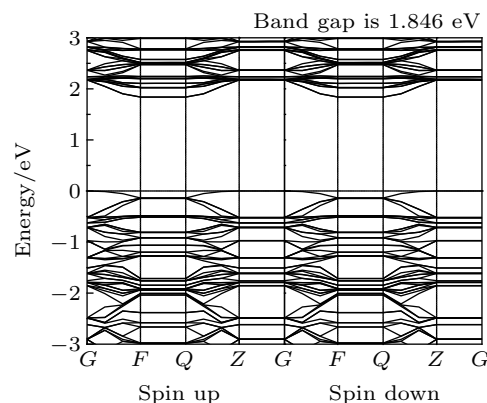


Fig. A1. Band structure of intrinsic MoS₂.

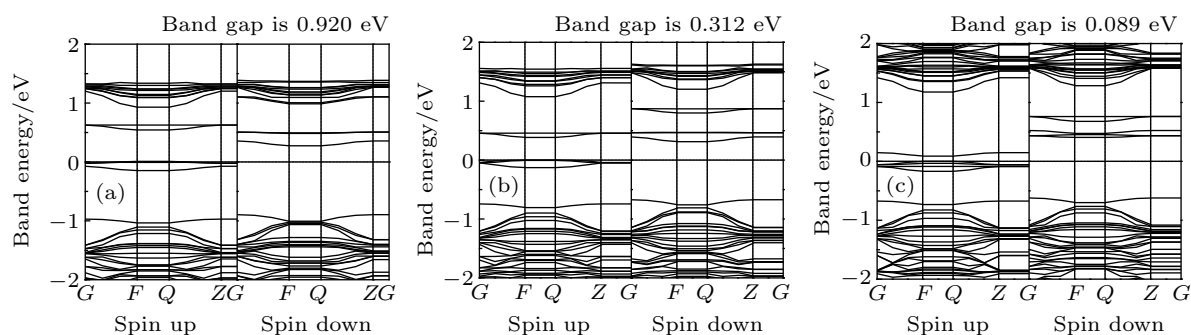


Fig. A2. Band structure for (a) Fe, (b) Co, (c) Ni-doped MoS₂.

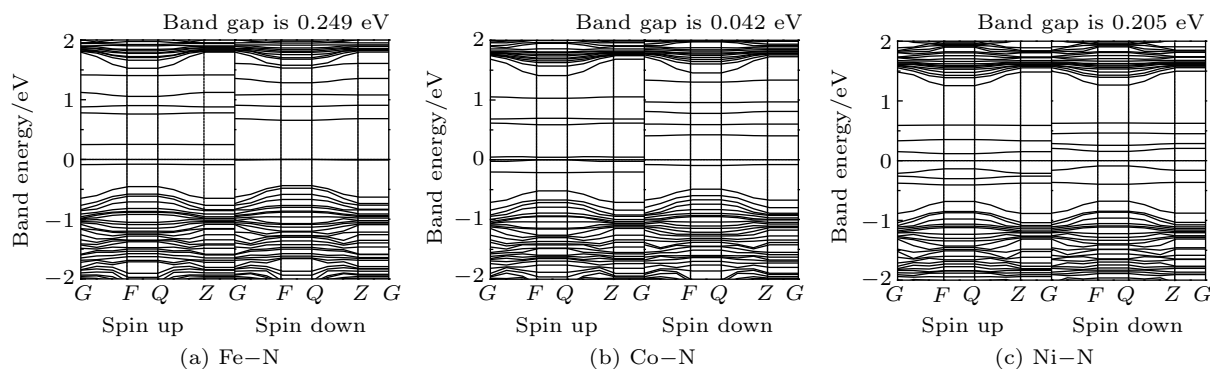


Fig. A3. Band structure of (a) Fe-N, (b) Co-N, and (c) Ni-N co-doped MoS₂.

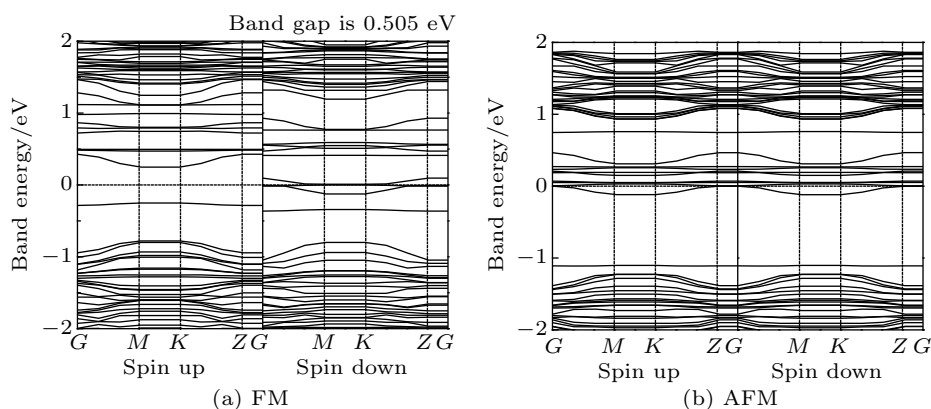


Fig. A4. Band structure of (2Fe, N) co-doped monolayer MoS₂: (a) FM, (b) AFM, respectively.

References

- [1] Castro Neto A H, Peres N M R, Novoselov K S and Geim A K 2009 *Rev. Mod. Phys.* **81** 109
- [2] Lucking M C, Xie W Y, Choe D H, West D, Lu T M and Zhang S B 2018 *Phys. Rev. Lett.* **120** 086101
- [3] Lu J P, Yang J, Carvalho A, Liu H, Lu Y R and Sow C H 2016 *Acc. Chem. Res.* **49** 1806
- [4] Li Y G, Li Y L, Sa B S and Ahuja R 2017 *Catal. Sci. Technol.* **7** 545
- [5] Feng Y P, Shen L, Yang M, Wang A Z, Zeng M G, Wu Q Y, Chintalapati S and Chang C R 2017 *WIREs. Comput. Mol. Sci.* **7** e1313
- [6] Kime G, Leontiadou M A, Brent J, Savjani N, O'Brien P and Binks D J 2017 *J. Phys. Chem. C* **121** 22415
- [7] Wen M, Xu J P, Liu L, Lai P T and Tang W M 2017 *IEEE Trans. Electron Dev.* **99** 1
- [8] Liu L, Wang X D, Han L, Tian B B, Chen Y, Wu G J, Li D, Yan M G, Wang T, Sun S, Shen H, Lin T, Sun J, Duan C, Wang J L, Meng X J and Chu J H 2017 *AIP Adv.* **7** 065121
- [9] Benavente E, Durán F, Sotomayor-Torres C and González G 2018 *J. Phys. Chem. Solids* **113** 119
- [10] Niefind F, Djamil J, Bensch W, Srinivasan B R, Sinev I, Grünert W, Deng M, Kienle L, Lotnyk A, Mesch M B, Senker J, Durag L and Beyerles T 2015 *RSC Adv.* **5** 67742
- [11] Cho B, Hahm M G, Choi M, Yoon J, Kim A R, Lee Y J, Park S G, Kwon J D, Kim C S, Song M, Jeong Y, Nam K S, Lee S, Yoo T J, Kang C G, Lee B H, Ko H C, Ajayan P M and Kim D H 2015 *Sci. Rep.* **5** 8052
- [12] Li Y, Cai C, Gu Y, Cheng W, Xiong W and Zhao C 2017 *Appl. Surf. Sci.* **414** 34
- [13] Xie Y, Zhang B, Wang S, Wang D, Wang A, Wang Z, Yu H, Zhang H, Chen Y, Zhao M, Huang B, Mei L and Wang J 2017 *Adv. Mater.* **29** 1605972
- [14] Radisavljevic B, Radenovic A, Brivio J, Giacometti V and Kis A 2011 *Nat. Nanotechnol.* **6** 147
- [15] Komsa H P, Kurasch S, Lehtinen O, Kaiser U and Krasheninnikov A V 2013 *Phys. Rev. B* **88** 1
- [16] Suh J, Tan T L, Zhao W, Park J, Lin D Y, Park T E, Kim J, Jin C, Saigal N, Ghosh S, Wong Z M, Chen Y, Wang F, Walukiewicz W, Eda G and Wu J 2018 *Nat. Commun.* **9** 1

- [17] Fan Y H, Zhang J Y, Qiu Y Z, Zhu J, Zhang Y F and Hu G L 2017 *Comput. Mater. Sci.* **138** 255
- [18] Zhang L Q, Liu T M, Li T F and Hussain S 2017 *Physica E* **94** 47
- [19] Ramasubramaniam A and Naveh D 2013 *Phys. Rev. B* **87** 1
- [20] Zhao H M 2016 *Joint International Information Technology, Mechanical and Electronic Engineering Conference*, October 4–5, 2016, Xi'an, China, p. 530
- [21] Cui H, Zhang X, Zhang G and Tang J 2019 *Appl. Surf. Sci.* **470** 1035
- [22] Cheriyan S, Balamurgan D and Sriram S 2018 *Superlattices Microstruct.* **116** 238
- [23] Garandel T, Arras R, Marie X, Renucci P and Calmels L 2017 *Phys. Rev. B* **95** 1
- [24] Cheng Y C, Zhu Z Y, Mi W B, Guo Z B and Schwingenschlgl U 2013 *Phys. Rev. B* **87** 100401(R)
- [25] Yue Q, Chang S, Qin S and Li J 2013 *Phys. Lett. A* **377** 1362
- [26] Lu S C and Leburton J P 2014 *Nanoscale Res. Lett.* **9** 676
- [27] Yiren W, Li-Ting Tseng, Peter P, Murmu, Nina Bao and John 2017 *Mater. Des.* **121** 77
- [28] Komsa H P, Kotakoski J, Kurasch S, Lehtinen O, Kaiser U and Krashennnikov A V 2012 *Phys. Rev. Lett.* **109** 35503
- [29] Dai Z, Jin W, Grady M, Sadowski J T, Dadap J I, Osgood R M and Pohl K 2017 *Surf. Sci.* **660** 16
- [30] Wu P, Yin N, Li P, Cheng W and Huang M 2017 *Phys. Chem. Chem. Phys.* **19** 20713
- [31] Lin L, Huang J, Yu W, Zhu L, Tao H, Wang P and Guo Y P 2019 *Solid State Commun.* **301** 113702
- [32] Guan L, Tan F X, Jia G Q, Shen G M, Liu B T and Li X 2016 *Chin. Phys. Lett.* **33** 087301
- [33] Dai X, Le C C, Wu X X, Qin S S, Lin Z P and Hu J P 2016 *Chin. Phys. Lett.* **33** 127301
- [34] Hu Y J, Xu S L, Wang H, Liu H, Xu X C and Cai Y X 2016 *Chin. Phys. Lett.* **33** 106102
- [35] Gu Y H, Feng Q, Chen J J, Li Y H and Cai C Z 2016 *Chin. Phys. Lett.* **33** 077102
- [36] Sun J P, Zhang D and Chang K 2017 *Chin. Phys. Lett.* **34** 027102
- [37] Liu P, Wang W H, Wang W C, Cheng Y H, Lu F and Liu H 2017 *Chin. Phys. Lett.* **34** 027101
- [38] Mak K F, Lee C, Hone J, Shan J and Heinz T F 2010 *Phys. Rev. Lett.* **105** 136805
- [39] Splendiani A, Sun L, Zhang Y, Li T, Kim J, Chim C Y, Galli G and Wang F 2010 *Nano Lett.* **10** 1271
- [40] Hu A M, Wang L L, Xiao W Z, Xiao G and Rong Q Y 2015 *Comput. Mater. Sci.* **107** 72
- [41] Jia C, Zhou B, Song Q, Zhang X and Jiang Z 2018 *RSC Adv.* **8** 18837